

THE COSMIC RAY DIFFERENTIAL DIURNAL VARIATION DEPENDENCES ON THE ZENITH ANGLE AND THE GEOMAGNETIC DISTURBANCE

S. Kavlakov and L. Georgiev

INSTITUTE FOR NUCLEAR RESEARCH AND NUCLEAR ENERGY,
BULGARIAN ACADEMY OF SCIENCES. SOFIA 1784. BULGARIA.

1. INTRODUCTION.

Simultaneous and continuous muon measurements in two opposite azimuthal directions under equal zenith angles III demonstrated the importance of this method for cosmic ray diurnal variation investigations. Lately these measurements were extended by means of improved telescopes I2,3I. The obtained cosmic ray diurnal variations were presented as intensity differential curves.

Theoretical investigations I4I connected the properties of these curves with some interplanetary space parameters. The harmonics of these curves were interpreted I5I physically. Second order difference curves were introduced I6I.

In our earlier works I7,8,9I some dependences between the parameters characterizing the first and the second harmonics of the differential intensity curves and the geomagnetic activity were found. Then all measurements were carried out under only one zenith angle.

Here we presented the results of investigations of similar dependences using data of simultaneous measurements under three different zenith angles.

2. EXPERIMENT.

The measurements were carried out on p. Musalá ($\varphi = 42^{\circ}11'N$; $\lambda = 23^{\circ}35'E$; $H = 2925$ m.a.s.l.) by means of a multi-directional counter telescope I10I. After the connection of a supplementary electronic circuit it became possible to measure simultaneously in the four cardinal azimuthal directions (East(E), West(W), North(N), South(S)) under three different zenith angles (40° ; 60° ; 70°) I11I.

On fig. 1. are shown the zenith angle sensitivities for the telescopes inclined under 40° ; 60° ; 70° .

On fig. 2. are plotted in polar coordinates the azimuth angle sensitivities for all our 12 telescopes measuring simultaneously.

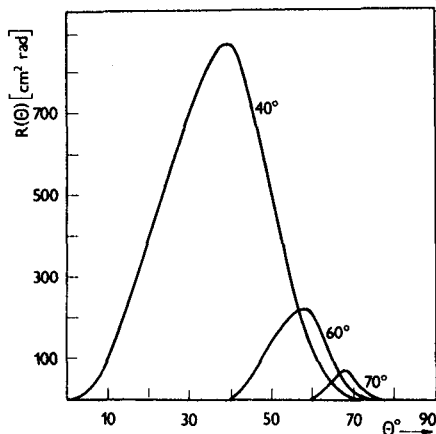


Fig. 1.

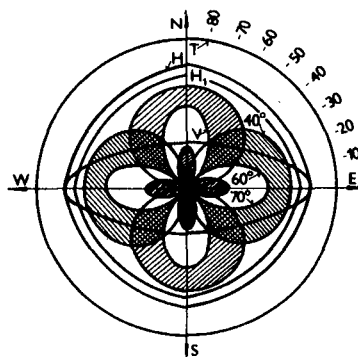


Fig. 2.

3. ASYMPTOTIC DIRECTIONS.

If the energy is sufficiently great the particle's primary direction does not change when it moves through the earth magnetosphere. On fig. 3. the small circles present the asymptotic directions ($\varphi_{E=\infty}, \lambda_{E=\infty}$) calculated following I12I for our telescopes and projected on the extended map of the Globe surface. There p. Musala is shown with a triangle.

The asymptotic directions for the same telescopes computed I13I for different lower energies are shown on the same figure as separate points. The points are connected with suitable curves for every one of the telescopes.

Because of the considerable width of the distributions of $R(\theta)$ and $P(\alpha)$ for the real telescopes, the points corresponding to all asymptotic direction projections for a certain energy cover a considerable area on the Globe surface. Then the curves plotted on fig. 3. form large strips.

It could be accepted that the differences of intensity data obtained simultaneously from two inclined telescopes, detecting under equal zenith angles in different azimuthal directions eliminate particles with energy below 18 - 20 GeV. So these differences are independent not only on meteorological changes, but on the changes in the low energy part of the cosmic ray spectrum.

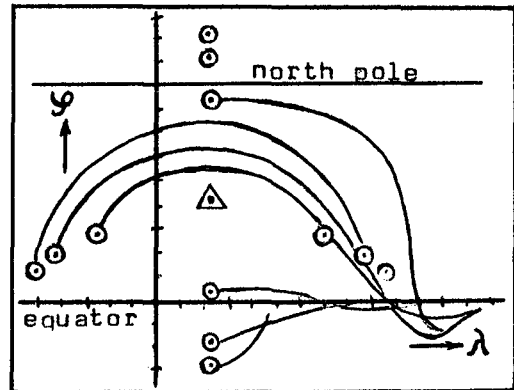


Fig. 3.

4. DATA TREATMENT.

From all the data obtained on p. Musala in the period June 1, 1981 - April 30, 1983 only "complete" data days were used. For these days all the 24 separate hourly measurements for all the 12 telescopes were available. From the measured hourly intensities for every separate day, for every separate zenith angle the following 8 differences were formed

I ordre: E - W; E - N; E - S; W - N; W - S; N - S;

II ordre: G = (N - S) - (E - N); K = (N - S) - (W - N).

To present the deviations in percentage around a zero average the formula

$$(1) \quad (E - W)_{ij} = 2 \frac{E_{ij} - W_{ij} - (\bar{E}_j - \bar{W}_j)}{\bar{E}_j + \bar{W}_j} 100\%$$

was used. Here i ($i = 1, 2, \dots, 24$) was the index of the i -hour measurement in the j -day. \bar{E}_j and \bar{W}_j are the corresponding daily averages. Analogically all other differences were formed.

To every one of the chosen days the indexes m and n were appropriate. So $j = j(m, n)$. The index m characterized the degree of the corresponding day magnetic activity. The values of m were chosen according I14I. The index n specified the continuity of the days around the beginning of the magnetic storm.

The combinations between m and n are classified on table 1.

Table 1.

	quiet $m = 0$	weak $m = 1$	moderate $m = 2$	intense $m = 3$	strong $m = 4$	All for the row
PRECEDING $n = -1$	—	1,-1	2,-1	3,-1	4,-1	$N = -1$
BEGINNING $n = 0$	—	1, 0	2, 0	3, 0	4, 0	$N = 0$
FOLLOWING $n = 1$	—	1, 1	2, 1	3, 1	4, 1	$N = 1$
For the column	—	$M = 1$	$M = 2$	$M = 3$	$M = 4$	MN

For every one of the three zenith angles ($40^\circ; 60^\circ; 70^\circ$), for every one of the 21 index combinations (table 1.) the average diurnal variation of every one of the 8 differences was investigated. Fourier analysis was applied for every one of these $3 \times 21 \times 8 = 504$ cases to compute the amplitudes $A_1; A_2; A_3$ (in percents) and the phases $t_1; t_2; t_3$ (in hours Local Solar Time (LST)) of the first (I), the second (II), and the third (III) harmonics.

5. RESULTS.

The first (I) and the second (II) harmonics for some of the computed differences for magnetically quiet days ($m = 0$), for the zenith angles $40^\circ, 60^\circ, 70^\circ$ are presented on fig. 4. as vector-hourly diagrams. The phases of the first harmonics remain grouped around 6 h.LST and the phases of the second harmonics - around 9 h.LST. That is valid for all the three zenith angles and practically for all other differences (not shown on the figure).

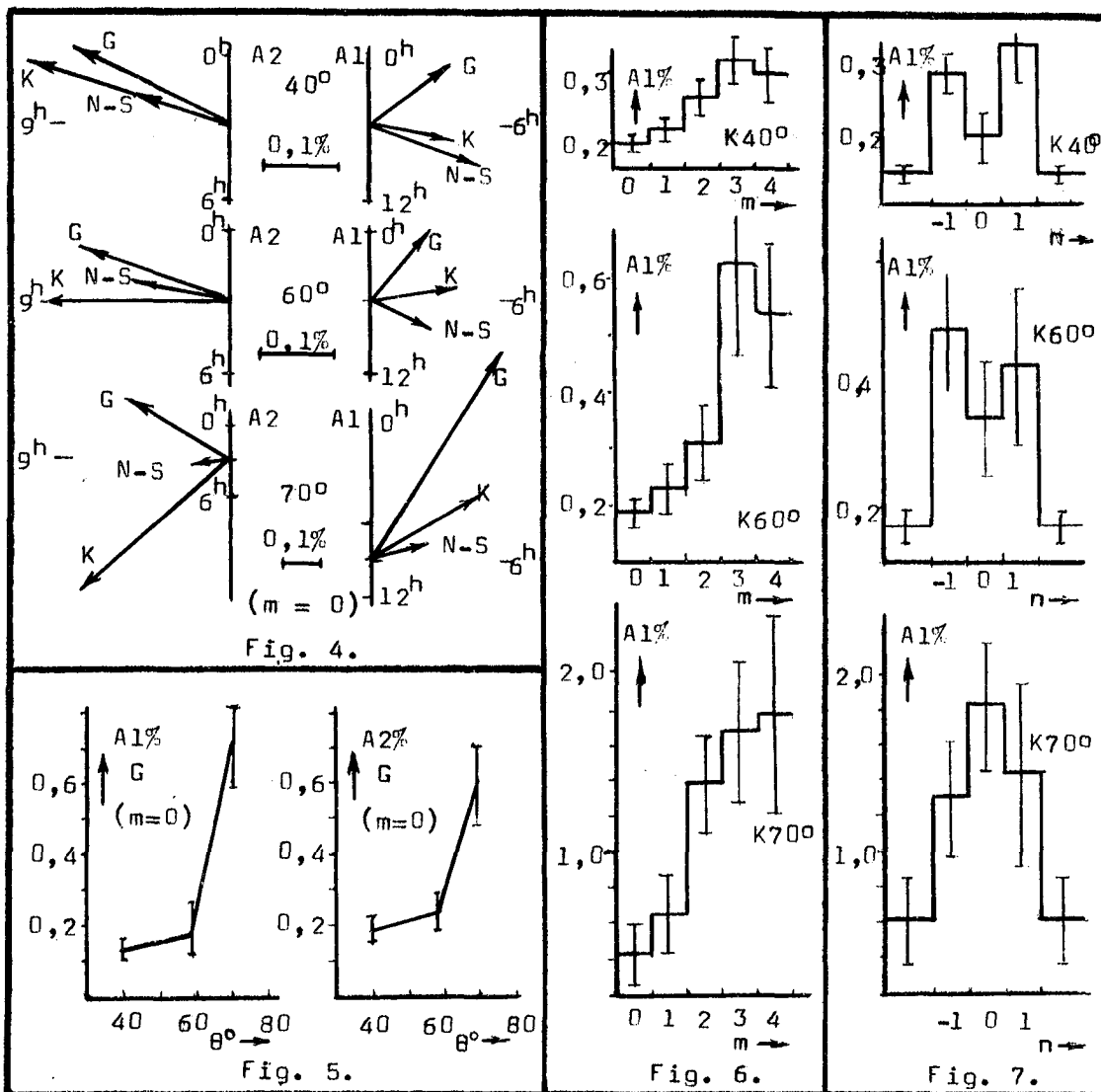
If these vectors are compared with those obtained 10 years ago on the same place, with the same apparatus (measuring then only under zenith angle of 60°) it could be assumed that they are rather stable in time

The amplitudes A_1 and A_2 increase with the zenith angle. As an example that is shown for G on fig. 5.

The first harmonic amplitude dependences on the magnetic disturbance degree are shown for K on fig. 6. for the three zenith angles. This amplitude, as well as the amplitudes of the other differences (not shown on the figure) increases with m . The increase is rather faster for greater zenith angles.

An interesting phenomena - the first harmonic amplitude increase in the days preceding the beginning of the magnetic storm observed in our earlier investigation I9I for zenith angle 60° , now is clearly expressed for all the three zenith angles ($40^\circ, 60^\circ, 70^\circ$). On fig. 7. are presented the changes of the first harmonic amplitude of the difference K in the days around the beginning of the magnetic storm compared with its value during magnetically quiet days. If the statistical accuracy of the separate diurnal measurement is sufficient then after a sudden jump in the amplitude's value, some short time forecast for a forthcoming magnetic disturbance could be done. This dependence is not well expressed for the second amplitudes.

In our case the third harmonics are generally small and their changes are practically in the limits of the statistical accuracy.



REFERENCES.

1. Kohlhörster W., Phys. Zs., 42 55 1941.
2. Elliot H., D. Dolbear, Proc. Phys. Soc., 63A 137 1950.
3. Sekido Y. et all. Multidirectional C.R.Intensity, Nagoya, 1975.
4. Nagashima K., Rep. Ionos. Space Res. Japan, 25/3 189 1971.
5. Nagashima K. et all., Rep. Ionos. Space Res. Japan, 26/1 1 1972.
6. Kondo I. et all., Proc. 14 ICRC München, 4 1182 1975.
7. Kavlakov S., Izv. Acad. Nauk USSR (Physics), 40/3 607 1976.
8. Kavlakov S., Proc. ICR Symp., Tokyo, 285 1976.
9. Kavlakov S., Proc. 15 ICRC, Plovdiv, 4 82 1977.
10. Kavlakov S., Compt. Rend. Acad. Bulg. Sci. 18/8 731 1965.
11. Kavlakov S., Thesis, Sofia, 1977.
12. Kavlakov S. et all. Proc. 17 ICRC, Paris, 4 237 1981.
13. Shea M. A. and D. F. Smart, Tables, Private communication.
14. Cosmic Data (in rushan) Moscau, 1981, 1982, 1983.